Structural asymmetry in the *Thermus thermophilus* RuvC dimer suggests a basis for sequential strand cleavages during Holliday junction resolution

Luan Chen, Ke Shi, Zhiqi Yin, Hideki Aihara*

Department of Biochemistry, Molecular biology and Biophysics, University of Minnesota, Minneapolis, MN 55455, USA

* To whom correspondence should be addressed. E-mail: aihar001@umn.edu

Abstract

Holliday junction (HJ) resolvases are structure-specific endonucleases that cleave four-way DNA junctions (Holliday junctions) generated during DNA recombination and repair. Bacterial RuvC, a prototype of HJ resolvase, functions as a homodimer and nicks DNA strands precisely across the junction point. To gain insights into the mechanisms underlying specific recognition of HJ DNA and symmetrical strand cleavages by RuvC, we performed crystallographic and biochemical analyses of RuvC from *Thermus thermophilus* (T.th. RuvC). The crystal structure of T.th. RuvC shows an overall protein fold similar to that of *Escherichia coli* RuvC, but T.th. RuvC has a more tightly associated dimer interface possibly reflecting its thermostability. The binding mode of a HJ-DNA substrate can be inferred from the shape/charge complementarity between the RuvC dimer and HJ-DNA, as well as positions of sulfate ions bound on the protein surface. Unexpectedly, the crystal structure of T.th. RuvC homodimer refined at 1.28Å resolution shows distinct asymmetry near the dimer interface, in the region harboring catalytically important aromatic residues. The observation suggests that the T.th. RuvC homodimer interconverts between two asymmetric conformations, with alternating subunits switched on for DNA strand cleavage. This model provides a structural basis for the "nick-counter-nick" mechanism in HJ resolution, a mode of HJ processing shared by prokaryotic and eukaryotic HJ resolvases.

Introduction

Homologous recombination plays critical roles in generating genetic diversity and repairing DNA lesions including double-strand breaks (West, 2003). A key intermediate formed during the homologous recombination process is a four-way junction DNA structure known as the Holliday junction (Holliday, 1964). In a Holliday junction, two homologous duplex DNA molecules are linked by single-stranded crossovers as a result of strand exchange. The Holliday junctions are resolved by structure-specific endonucleases called Holliday junction resolvases that cleave the two crossover strands across the junction point (Bennett et al., 1993; Eggleston and West, 2000). The enzymatic resolution of Holliday junction ensures that the canonical linear double-stranded DNA structure is restored upon completion of the recombination reaction, which is critical for the DNA molecules to segregate at cell division. Holliday junctions formed by replication fork reversal, a mechanism for rescuing stalled forks during DNA replication, are also resolved by Holliday junction resolvases. Thus, Holliday junction resolvases are important in maintaining genome integrity, and are found across all kingdoms of life from bacteriophages to humans.

In most bacteria, Holliday junctions are processed by the RuvA, RuvB and RuvC proteins originally identified through mutations that confer genetic defects in UV-induced DNA damage repair (Shinagawa and Iwasaki, 1996; West, 1997; Sharples et al., 1999). The RuvA-RuvB complex facilitates an ATP-dependent branch migration of Holliday junction, modulating the size of the hetroduplex region during homologous recombination (Shiba et al., 1991; Iwasaki et al., 1992; Parsons et al., 1992; Tsaneva et al., 1992). According to a proposed model, two homologous duplex arms in a four-way junction exchange their pairing partners by an unwinding-rewinding process when passing through the RuvA octamer (Parsons et al., 1995), while RuvB complex functions as a pump to pull DNA duplex arms. The branch migration allows relocation of the junction point to any cleavable sequences. RuvC, the Holliday junction resolvase, then resolves the Holliday junction structure into duplex products via a pair of symmetrical incisions across the junction point (Davis and West, 1998; Ichiyanagi et al., 1998). The dual incisions turn the Holliday junctions into two

nicked duplex products that can be directly repaired by DNA ligases (Dunderdale et al., 1991; Iwasaki et al., 1991).

Even though the *E. Coli* RuvC binds to Holliday junction DNA in a sequence non-specific fashion, it exhibits sequence selectivity in DNA cleavage and preferentially nicks at 3' side of Thy bases (Shida et al., 1996; Shah et al., 1994). It has been suggested that the rate-limiting step during Holliday junction resolution is the first strand cleavage; once RuvC nicks one strand, it quickly cuts the opposing strand to complete the resolution reaction (Fogg and Lilley, 2000; Osman et al., 2009). Thus, Holliday junction resolution by RuvC entails two sequential strand cleavages. Similarly, eukaryotic Holliday junction resolvases cut pre-nicked Holliday junctions much more readily than intact HJ substrate, suggesting that the "nick-counter-nick" mechanism may be a common strategy employed by HJ resolvases. The molecular bases for the sequence selectivity and the asymmetric sequential DNA cleavages are not well understood.

The crystal structure of the RuvC resolvase from *E.coli* at 2.5Å resolution (Ariyoshi et al., 1994) revealed that RuvC forms a symmetric homodimer of 19kDa subunits with an elongated overall shape. The catalytic center of each subunit is composed of four acidic residues, Asp7, Glu66, Asp138 and Asp141, clustered at the bottom of a basic cleft (Saito et al., 1995). These carboxylate residues coordinate divalent metal cations such as Mg^{2+} and Mn^{2+} to catalyze hydrolysis of the phosphodiester bond in DNA backbones, which is a common feature shared by many endonucleases (Takahagi et al., 1994; Saito et al., 1995; Yang, 2011). The two catalytic centers in the RuvC dimer are positioned on the same side of a dimer surface, defining the "front" side of the enzyme responsible for the DNA-binding. The region between the two active centers on the surface of the RuvC dimer includes Phe69, a residue critical in the Holliday junction binding and resolution (Ichiyanagi et al., 1998; Yoshikawa et al., 2001). During junction cleavage by RuvC, the aromatic ring of phenylalanine 69 is thought to stack on a DNA nucleobase and stabilize the open square-planner conformation of Holliday junction to facilitate its resolution.

Even though the *E. Coli* RuvC has long served as a model system of Holliday junction resolvase, mechanisms of Holliday junction recognition and symmetrical strand cleavages by RuvC are not fully

understood. Despite the importance of RuvC in DNA recombination and repair across prokaryotes, there is essentially no biochemical study reported for RuvC from bacteria other than *E coli*, and the crystal structure of the E. Coli RuvC (Ariyoshi *et al*., 1994) remains to be the only structure of RuvC from any organism. We reasoned that additional high resolution structural information would help better understand how RuvC specifically recognizes and resolves Holliday junction DNA, and performed crystallographic studies of RuvC from *Thermus thermophilus*. Structural information on T.th RuvC could also reveal structural differences among RuvC orthologs that may contribute to their unique biochemical properties.

Methods and materials

Purification of *T. thermophilus* RuvC protein

Codon-optimized synthetic gene for the *Thermus thermophilus* RuvC protein was inserted into the pET11a vector to generate the expression plasmids used in this study. The expression plasmids for the D146N, F73A, F74A, and Y75A point mutants were generated by the standard site-directed mutagenesis procedure. The proteins were overexpressed in *E coli* BL21(DE3). Transformed bacterial cells were grown in 4L of LB medium supplemented with 0.4g ampicillin to an OD_{600} of ~0.5, at which point isopropyl-β-D-thio-galactoside (IPTG) was added to a final concentration of 1mM to induce protein expression. The cells were further incubated at 20^{o}C for 18 hours and then collected by centrifugation. The collected cells were re-suspended in 40ml of buffer A (20mM HEPES-NaOH pH7.5, 0.25M NaCl), disrupted by sonication, and spun at 59,000 x g for 1 hour. The supernatant was then heated at 70^{o}C for 30 minutes and centrifuged again at 59,000 x g for 40 minutes. The supernatant was filtered through a surfactant-free cellulose acetate (SFCA) membrane with 0.2μm pore-size. The filtered supernatant was then applied onto a Hi-trap Heparin-Sepharose column pre-equilibrated with buffer A. Elution by a linear NaCl gradient yielded a single peak corresponding to the purified RuvC protein.

Protein-DNA binding assay

A HJ-DNA substrate with alternating 10bp and 14bp arms was mixed with various amounts of T.th. RuvC in buffer A, yielding the ratios between HJ- DNA and RuvC protein dimer ranging from 0.125 to 1.125. The reaction mixtures were then mixed with equivalent volumes of loading buffer (10mM HEPES pH7.5, 10% glycerol and 0.1%w/v bromophenol blue indicator), giving the final DNA concentration of 0.01 mM. 10ul of each reaction mixtures were then applied to a 10% polyacrylamide-TBE (Tris-Borate-EDTA) gel. Electrophoresis was performed at room temperature at 100V/8cm for approximately 1 hour in a running buffer containing 1/2X TBE buffer. The gel was first stained with ethidium bromide to visualize DNA then stained with Coomassie brilliant blue to visualize protein.

HJ-DNA resolution assay

The reaction mixture (50 µl) containing 6-FAM labeled synthetic DNA junction (100 nM) and T.th. RuvC (500 nM or 1.0µM) in 20 mM HEPES-NaOH (pH 7.5), 50 mM NaCl, 5 mM $MnCl_2$, 1 mM TCEP, 5% (v/v) Glycerol and 15% (v/v) DMSO was incubated for 60 min at 58 ^{o}C. The reactions were stopped by the addition of 1 µl 10% SDS and 50 µl denaturing PAGE gel-loading buffer (95% Formamide and 0.25% Bromophenol Blue), denatured by heating, and analyzed by 15% polyacrylamide TBE-Urea gels (Invitrogen). The gels were scanned by a FUJIFILM Fluorescent Image Analyzer. The sequences of the oligonucleotides used to form the HJ substrate were as follows. FAM_RUV_X64_1 (5'-ATTCTACCAG TGCCTTGCTA GCCACAGCCA GTCAGCCGAT TGCGGGACAT CTTTGCCCAC CTGC-3'), RUV_X64_2 (5'-GCAGGTGGGC AAAGATGTCC CGCAATCGGC TGAGACCGAG CACGATCTGT TGTAATCGTC AAGC-3'), RUV_X64_3 (5'-GCTTGACGAT TACAACAGAT CGTGCTCGGT CTCTCGGCAG ATGCCATGGA GCTGTCTAGA GGAT-3'), RUV_X64_4 (5'-ATCCTCTAGA CAGCTCCATG GCATCTGCCG AGACTGGCTG TGGCTAGCAA GGCACTGGTA GAAT-3'). This substrate is a "bimobile" HJ junction (Shida, et al., 1996) with limited central mobility.

Crystallization

The T.th. RuvC crystals were grown by the hanging drop vapor diffusion method at 20^{o}C. The wild-type RuvC crystals (form I) were obtained by mixing the protein at ~2mg/mL in 20mM HEPES (pH7.5), 0.25M NaCl and 2.5mM 2-mercaptoethanol with an equal volume of well solution consisting of 35% polyethylene glycol (PEG) 3,350, 0.2M Li_2SO_4, and 0.1M Tris-HCl (pH8.5). Crystals typically appeared after ~48 hours and continued to grow for a week. The crystals were cryoprotected by gradually introducing glycrol into the drops to a final concentration of 20% then flash frozen in liquid nitrogen. X-ray diffraction data were collected at the beamlines 24ID-C and 24ID-E (Advanced Photon Source, Argonne IL). The crystals visually appeared to be single but turned out to be clusters of smaller crystals. Thus, datasets were collected by shooting corners of crystals with an x-ray beam collimated to a 10μm diameter. Best crystal diffracted to a Bragg spacing of ~1Å. The crystal belonged to the space group $P2_12_12_1$, with the unit cell parameters of 36.7Å, 51.1Å, 134.7Å. The asymmetric unit contained two RuvC molecules.

For the D146N RuvC crystals (form II), the well solution consisted of 32% PEG400, 0.4M Li2SO4, and 0.1M sodium acetate (pH4.2). Although crystallization in this condition required the presence of a HJ DNA substrate, we did not observe a bound DNA in the final electron density map. The crystals belonged to the space group $I2_12_12_1$, with the unit cell parameters of 35.2Å, 60.0Å, 135.7Å. The asymmetric unit contained a RuvC monomer.

Structure determination and refinement

X-ray diffraction frames were processed using the HKL2000 suite (Otwinowski and Minor, 1997). A molecular replacement calculation was performed with PHASER (McCoy et. al., 2007) on the higher resolution wild-type *T.th.* RuvC dataset (crystal form I) using the *E. coli* RuvC as the search model, yielding a clear solution. Iteration of phase-restrainted refinement using REFMAC5 (Murshudov et. al., 1997) and manual model building in COOT (Emsley et. al., 2004) eventually generated a model consisting of residues 1 ~ 166 for two T.th. RuvC molecules and 414 water molecules. The final model has been refined at 1.28Å resolution to a free R-factor of 19.5% using PHINEX (Adams et. al., 2010). No non-crystallographic

symmetry restraint was used throughout the refinement. The structure of the D146N mutant (form II) was determined employing the refined *T.th.* RuvC model from the form I as the molecular replacement search model, and was refined to a final free R-factors of 29.4% at 2.08Å resolution.

Results and Discussion

We purified the recombinantly expressed full-length *Thermus thermophilus* RuvC, and demonstrated that it functions as a HJ-DNA resolvase *in vitro*. T.th. RuvC cleaved DNA strands at specific positions in a synthetic HJ-DNA substrate with limited mobility of the branch point (Figure 1). Similarly to *E. coli* RuvC (Osman *et. al*., 2009), T.th. RuvC also exhibited the resolvase activity on a pre-nicked HJ-DNA in which one of the four strands is nicked at the branch point, provided that the 5'-end of DNA at the nick is phosphorylated (data not shown). We found the optimal reaction temperature for T.th. RuvC in our assay to be 58^{o}C. No endonuclease activity was detected at 37^{o}C, confirming that the observed activities were not due to a contaminating *E. coli* enzyme. The D146N mutant that has a mutation in one of the catalytic carboxylate residues showed no HJ resolvase activity (Figure 1).

We have determined crystal structures of the *Thermus thermophilus* RuvC HJ resolvase in two different crystal forms at 1.28Å and 2.0Å resolution. The first crystal form that gave the higher resolution diffraction (form I; Figure 2) was obtained with the wild-type T.th. RuvC and PEG3350 as the precipitant, and contained one RuvC homodimer in the asymmetric unit. The two protein molecules in the RuvC homodimer are related by a pseudo 2-fold axis but deviate from the perfect symmetry. The second crystal form, obtained with the D146N mutant and PEG400 as the precipitant (form II), had one RuvC molecule in the asymmetric unit and thus the RuvC homodimer obeys a perfect 2-fold symmetry. Molecular packing arrangements in the two crystal forms are otherwise similar to each other.

T.th. RuvC has a protein fold consisting of a single layer of β-sheet sandwiched between α-helices, characteristic of enzymes from the retrovirus integrase superfamily (Figure 3) (Nowotny, 2009). The overall

structure of the T. th. RuvC homodimer is similar to that of E. coli RuvC, as expected from the reasonably high amino acid sequence identity (~35%) between the two proteins (Figure 4). The RuvC homodimers from *E. Coli* and T.th. can be superimposed with an r.m.s.d. for the backbone Cα atoms of 1.6Å (over 130 atoms per monomer). The structural deviations are attributed mostly to the loop regions between the secondary structure elements, and the N- and C-termini of the protein. For instance, in contrast to the flexible C-terminal end of *E. Coli* RuvC, the C-terminus of T.th. RuvC is fully ordered with the last residue Leu166 involved in dimerization interactions. The terminal carboxyl group of Leu166 forms a hydrogen bond with the backbone amide group of Ala44 from the other molecule, while its sidechain is part of the hydrophobic dimer interface. Although many of the secondary structure elements superimpose very well between the *E. Coli* and T.th. RuvC dimers, notable differences were found in the positions of the long α-helices in the core of the protein dimer (α-helices A and B) such that the T.th. RuvC has a more tightly associated dimer interface (Figure 4). This is reflected in the difference in total buried accessible surface areas at the dimer interface, 1896Å^2 for *E. Coli* RuvC versus 2432Å^2 for *T.th.* RuvC. In addition, the dimer interface of T.th. RuvC is richer in aromatic residues with Tyr82, Trp86, and Phe96 involved in the hydrophobic interactions (Figure 5). These structural differences may account for the improved thermostability of T.th. RuvC.

The catalytic center of T.th. RuvC is composed of Asp7, Glu70, His143, and Asp146, clustered at the bottom of a cleft that traverses the protein surface (Figure 6). The third metal-chelating residue in the primary sequence, corresponding to Asp138 of *E.coli* RuvC, is a histidine (His143) in T.th. RuvC. Having histidine at this position is a feature shared by many RuvC orthologs according to the sequence alignment (not shown). Based on analogy to other enzymes in the retroviral integrase family such as RNaseH1 (Nowotny and Yang, 2006) the tetrad of active site residues are expected to chelate two metal ions to catalyze hydrolysis of DNA backbone phosphodiester bonds. The active centers of T.th. RuvC are

surrounded by broad positively charged surfaces, as expected for an enzyme known to bind DNA in a sequence non-specific fashion.

Based on the overall shape, surface electrostatic potential, and the location of the enzyme active site on the T.th. RuvC dimer, the mode of its HJ-DNA binding can be readily predicted. We therefore built a hypothetical model of how the T.th. RuvC dimer binds a Holliday junction DNA (Figure 7). In the structure of T.th. RuvC crystallized in a higher concentration of Li_2SO_4 (crystal form II) refined at 2.0Å resolution, a total of 4 sulfate ions per RuvC monomer were found to be bound on the protein surface. Two of these four sulfate ions are located along the edge of the basic cleft harboring the catalytic residues, likely mimicking backbone phosphate groups of a bound DNA. Thus the paths of DNA strands in the RuvC-HJ DNA model were adjusted guided by these sulfate positions. The bound Holliday junction in the resulting model assumes the open square-planer conformation, consistent with predictions from earlier biochemical studies and docking models (Ariyoshi et al., 1994; Yoshikawa et al., 2001).

Unexpectedly, the structure of the T.th RuvC homodimer refined at 1.28Å resolution shows distinct asymmetry in residues 73 to 81 that span the dimer interface (Figure 8). This region, comprising the N-terminus of α-helix B and the preceding loop, forms a lobe (referred to as "wall" in earlier publications) located between the two active centers on the surface of the RuvC dimer. The lobe fits into the central opening of the Holliday junction DNA in our model of the T.th. RuvC-HJ DNA complex. In one of the molecules within the RuvC dimer, the α-helix B starts from Ala81and the preceding loop projects into/over the active site cleft. In the other molecule, the helix starts from Glu79 and the preceding residues are positioned farther from the active site. The asymmetric conformations of these residues are stabilized by intermolecular as well as intramolecular hydrogen-bonds formed by Gln77. The corresponding region in the strictly 2-fold symmetrical RuvC homodimer (form II) appears to be disordered, as the 2.0Å resolution 2Fo-Fc map does not show interpretable electron density. Taken together, these observations suggest that the residues 73 to 81 of T.th. RuvC interconvert between two alternate conformations in a concerted fashion

within the protein dimer to break the 2-fold symmetry. This "flip-flop" motion has an important implication in the mechanism of Holliday junction resolution as discussed below.

The presence of sequence selectivity in DNA strand cleavage by *E. Coli* RuvC suggests that RuvC makes base contacts near the cutting site. Phe69 of *E. Coli* RuvC has been proposed to play a critical role in base-stacking near the junction point, based on the observation that F69A mutation causes severe defect in HJ resolution (Yoshikawa, et al., 2001). The corresponding residue Phe73 of T.th. RuvC is located in the loop region that undergoes the conformation switch, projecting into the active-site cleft in one of the molecules within the dimer while pointing away from the active site and partially buried in the other molecule. In our model of the T.th. RuvC dimer bound to a Holliday junction DNA, Phe73 from one of the molecules is positioned in close proximity to DNA poised for making base-stacking interaction. Curiously, Phe73 of T.th. RuvC is followed by Phe74 and Tyr75, where these aromatic residues all take different conformations between the two molecules in the dimer (Figure 8). It is tempting to speculate that some or all of these aromatic residues (Phe73, Phe74, Tyr75) play roles in positioning DNA during the strand cleavage, and only one of the molecules within the T.th. RuvC dimer can have a productive active site for DNA cleavage at a given time. We therefore tested the in vitro HJ-DNA cleavage activities of T.th. RuvC with point mutations, F73A, F74A, or Y75A. The three mutant proteins showed an interesting spectrum of activities (Figure 1). F73A showed a moderate defect in HJ-DNA processing, although it was not completely inactive like the corresponding F69A mutant of *E. coli* RuvC. F74A cleaved DNA but at a different position compared to the wild-type, suggesting altered structure/sequence selectivity. Y75A appeared to be hyperactive, and cleaved DNA more efficiently than the wild-type. The results are consistent with the idea that these aromatic residues are involved in DNA interactions near the scissile site, modulating DNA cleavage by T.th. RuvC.

It was shown previously that the two enzyme active sites within the RuvC dimer can operate independently of each other (Shah et al., 1997) and the resolution of a Holliday junction DNA by RuvC is likely achieved by two sequential, symmetrical strand cleavages across the junction point (Fogg and Lilley,

2000; Osman et. al., 2009). Our work raises an intriguing possibility that the two active sites in the T.th. RuvC dimer may be in fact not either concerted or independent of each other. Rather, the two molecules switch roles *via* concerted conformational changes (flip-flop motion) during the sequential strand cleavages. The local structural asymmetry and flexibility in an otherwise 2-fold symmetrical Holliday junction resolvase dimer could be a common theme for broader classes of Holliday junction resolvases including those from eukaryotic organisms that employ the "nick-counter-nick" mechanism in Holliday junction resolution.

Acknowledgements

We thank staffs at the Sector-24 (NE-CAT) of the Advanced Photon Source (APS) for help in x-ray data collection. Computer resources were provided by the Basic Sciences Computing Laboratory of the University of Minnesota Supercomputing Institute. This work is based upon research conducted at the APS on the NE-CAT beamlines, which are supported by award RR15301 from the National Center for Research Resources at the National Institutes of Health. Use of the Advanced Photon Source, an Office of Science User Facility operated for the U.S. Department of Energy (DOE) Office of Science by Argonne National Laboratory, was supported by the U.S. DOE under Contract No. DE-AC02-06CH11357. Supported by NIH grant GM095558 (to H.A.) and a funding from the Undergraduate Research Opportunity Program of the University of Minnesota (to L.C.).

Accession numbers

The atomic coordinates and structure factors have been deposited in the Protein Data Bank with the accession codes 4EP4 (form I) and 4EP5 (form II).

References

1. Ariyoshi M, Vassylyev DG, Iwasaki H, Nakamura H, Shinagawa H, Morikawa K. (1994). Atomic structure of the RuvC resolvase: a holliday junction-specific endonuclease from E. coli. Cell 78(6):1063-72.

2. Bennett RJ, Dunderdale HJ, West SC. (1993) Resolution of Holliday junctions by RuvC resolvase: cleavage specificity and DNA distortion. Cell.;74(6):1021-31.

3. Dunderdale, H.J., Benson, F.E., Parsons, C.A., Sharples, G.J., Lloyd, R.G. & West, S.C. (1991) Formation and resolution of recombination intermediates by E. coli RecA and RuvC proteins. Nature 354, 506–510.

4. Davies,A.A&West,S.C.(1998) Formation of RuvABC-Holliday junction complexes in vitro. Curr. Biol. 8, 725–727.

5. Eggleston AK, West SC.J. (2000) Cleavage of holliday junctions by the Escherichia coli RuvABC complex. Biol Chem.;275(34):26467-76.

6. Fogg JM, Lilley DM. (2000) Ensuring productive resolution by the junction-resolving enzyme RuvC: large enhancement of the second-strand cleavage rate. Biochemistry ;39(51):16125-34.

7. Holliday, R. 1964. A mechanism for gene conversion in fungi. Genet. Res. 5, 282–304

8. Nowotny, M. and Yang, W. (2006) Stepwise analyses of metal ions in RNase H catalysis: from substrate destabilization to product release EMBO J.(25): 1924-33.

9. Nowotny, M. (2009) Retroviral integrase superfamily: the structural perspective. EMBO reports.144 - 151 doi:10.1038/embor.2008.256

10. Ichiyanagi K, Iwasaki H, Hishida T, Shinagawa H.Mutational analysis on structure-function relationship of a holliday junction specific endonuclease RuvC. (1998) Genes Cells.;3(9):575-86.

11. Ip, S.C., Rass, U., Blanco, M.G., Flynn, H.R., Skehel, J.M., West, S.C. (2008) Identification of Holliday junction resolvases from humans and yeast. Nature.456(7220):357-61.

12. Iwasaki, H., Takahagi, M., Shiba, T., Nakata, A. & Shinagawa, H. (1991) Escherichia coli RuvC protein is an endonuclease that resolves the Holliday structure. EMBO J. 10, 4381–4389.

13. Iwasaki, H., Takahagi, M., Nakata, A. & Shinagawa, H. (1992) Escherichia coli RuvA and RuvB proteins specifically interact with Holliday junctions and promote branch migration. Genes Dev. 6, 2214±2200.

14. Osman F, Gaskell L, Whitby MC (2009) Efficient Second Strand Cleavage during Holliday Junction Resolution by RuvC Requires Both Increased Junction Flexibility and an Exposed 5′ Phosphate. PLoS ONE 4(4): e5347. doi:10.1371/journal.pone.0005347

15. Parsons, C.A., Tsaneva, I., Lloyd, R.G. & West, S.C. (1992) Interaction of Escherichia coli RuvA and RuvB proteins with synthetic Holliday junctions. Proc. Natl. Acad. Sci. USA 89, 5452 – 5456.

16. Parsons, C.A., Stasiak, A., Bennett, R.J. & West, S.C. (1995) Structure of a multisubunit complex that promotes DNA branch migration. Nature 374, 375±378.

17. Saito, A., Iwasaki, H., Ariyoshi, M., Morikawa, K. & Shinagawa, H. (1995) Identification of four acidic amino acids that constitute the catalytic center of the RuvC Holliday junction resolvase. Proc. Natl. Acad. Sci. USA 92, 7470-7474.

18. Shah, R., Bennett, R.J. & West, S.C. (1994) Genetic recombination in E. coli: RuvC protein cleaves Holliday junctions at resolution hotspots in vitro. Cell 79, 853–864.

19. Shah R, Cosstick R, and West S C. (1997) The RuvC protein dimer resolves Holliday junctions by a dual incision mechanism that involves base-specific contacts. EMBO; 16(6): 1464–1472. doi: 10.1093/emboj/16.6.1464

20. Sharples, G.J., Ingleston, S.M. & Lloyd, R.G. 1999. Holliday junction processing in bacteria: insights from the evolutionary conservation of RuvABC, RecG, and RusA. J Bacteriol 181: 5543-5550.

21. Shiba, T., Iwasaki, H., Nakata, A. & Shinagawa, H. (1991) SOS- inducible DNA repair proteins, RuvA and RuvB, of Escherichia coli: functional interactions between RuvA and RuvB for ATP hydrolysis and renaturation of the cruciform structure in supercoiled DNA. Proc. Natl. Acad. Sci. USA 88,
8445±8449.

22. Shida, T., Iwasaki, H., Saito, A., Kyogoku, Y. & Shinagawa, H. (1996) Analysis of substrate specity of the RuvC Holliday junction resolvase with synthetic Holliday junction. J. Biol. Chem. 42, 26105±26109.

23. Shinagawa, H. & Iwasaki, H. (1996) Processing the Holliday junction in homologous recombination. Trends Biol. Sci. 21, 107 – 111.

24. Takahagi, M., Iwasaki, H. & Shinagawa, H. (1994) Structural requirements of substrate DNA for binding to and cleavage by RuvC, a Holliday junction resolvase. J. Biol. Chem. 269, 15132 – 15139.

25. Tsaneva, I.R., MuÈller, B. & West, S.C. (1992) ATP-dependent branch migration of Holliday junctions promoted by the RuvA and RuvB proteins of E. coli. Cell 69, 1171±1180.

26. West, S.C. (1997) Processing of recombination intermediates by the RuvABC proteins. Annu. Rev. Genet. 31, 213–244.

27. West SC. (2003) Molecular views of recombination proteins and their control. Nat Rev Mol Cell Biol. 4(6):435-45.

28. Yang, W. (2011) Nucleases: diversity of structure, function and mechanism. *Q. Rev. Biophys*. **44**, 1-93.

29. Yoshikawa M, Iwasaki H, Kinoshita K, Shinagawa H. 2000. Two basic residues, Lys-107 and Lys-118, of RuvC resolvase are involved in critical contacts with the Holliday junction for its resolution. Genes Cells;5(10):803-13.

30. Yoshikawa M, Iwasak H, and Shinagawa H. (2001). Evidence that Phenylalanine 69 in Escherichia coli RuvC Resolvase Forms a Stacking Interaction during Binding and Destabilization of a Holliday Junction DNA Substrate. J. Biol. Chem., Vol. 276, Issue 13, 10432-10436

31. Otwinowski, Z., Minor, W. (1997) Processing of x-ray diffraction data collected in oscillation mode. *Methods Enzymol*. **276**, 307-326.

32. Murshudov, G.N., Vagin, A.A., Dodson, E.J. (1997) Refinement of macromolecular structures by the maximum-likelihood method. *Acta Cryst.* **D53**, 240-255.

33. Emsley, P., Cowtan, K. (2004) Coot: model-building tool for molecular graphics. *Acta Cryst.* **D60**, 2126-2132.

34. McCoy, A. J., Grosse-Kunstleve, R. W., Adams, P.D., Winn, M.D., Storoni, L.C., Read, R.J. (2007) Phaser crystallographic software. *J. Appl. Cryst.* **40**, 658-674.

35. Adams, P. D., Afonine, P.V., Bunkóczi, G., Chen, V. B., Davis, I. W., Echols, N., Headd, J. J., Hung, L. W., Kapral, G. J., Grosse-Kunstleve, R. W., McCoy, A. J., Moriarty, N. W., Oeffner, R., Read, R. J., Richardson, D. C., Richardson, J. S., Terwilliger, T. C., Zwart, P. H. (2010) PHENIX: a comprehensive Python-based system for macromolecular structure solution. *Acta Cryst.* **D66**, 213-221.

Figures

Figure 1 | *Thermus thermophilus* RuvC functions as a Holliday junction resolvase *in vitro*.

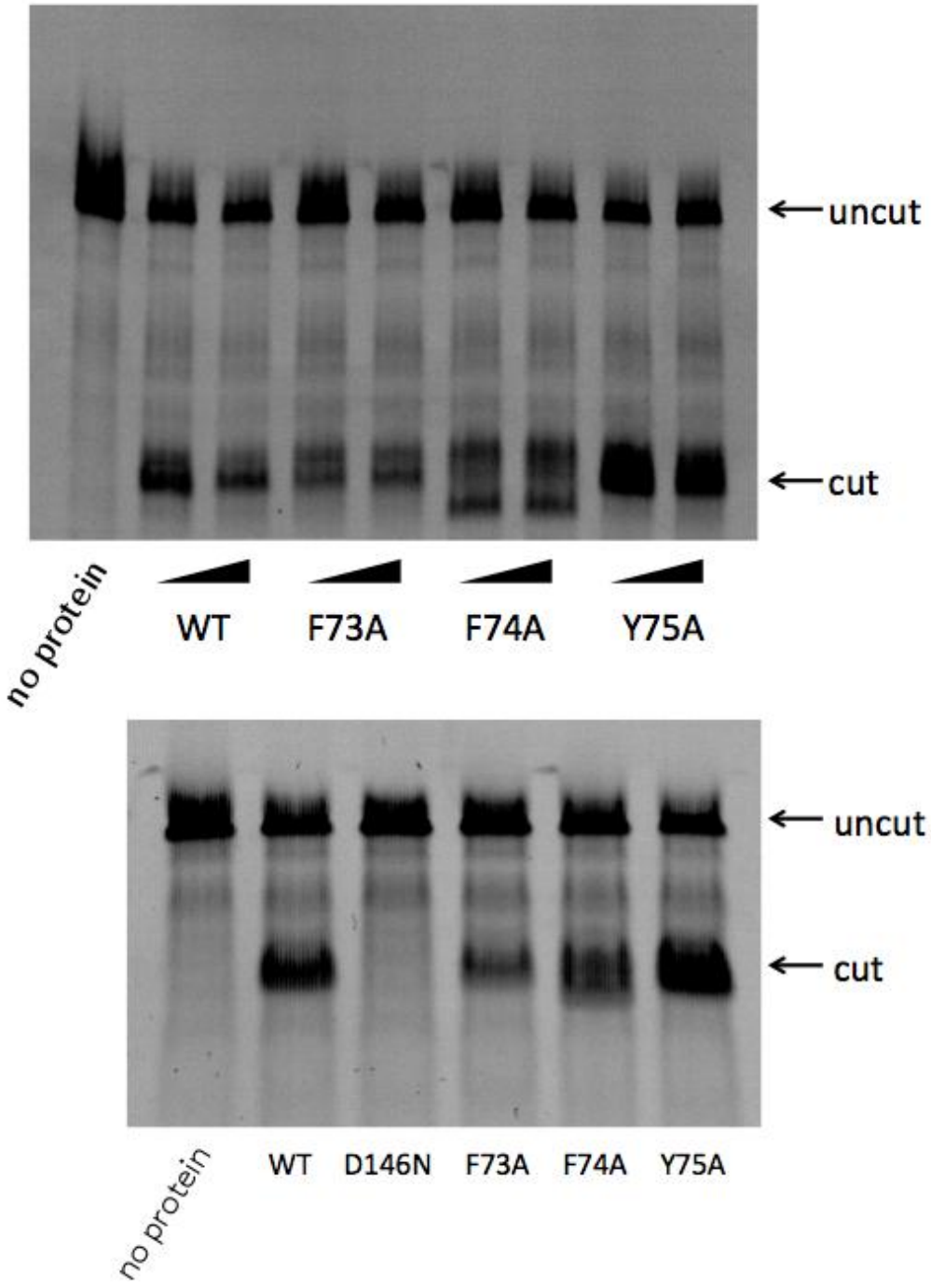

The HJ-DNA resolution assay on the wild-type and mutant T.th. RuvC proteins. The top band corresponds to the uncut 64-base oligonucleotide, and the bottom bands correspond to the cleaved products. The mutation of a catalytic residue Asp146 abolishes the DNA cleavage activity whereas mutations of the

aromatic residues in the asymmetric loop region differently modulate the HJ resolvase activity.

Figure 2 | T.th. RuvC crystal diffracts x-ray to a high resolution.

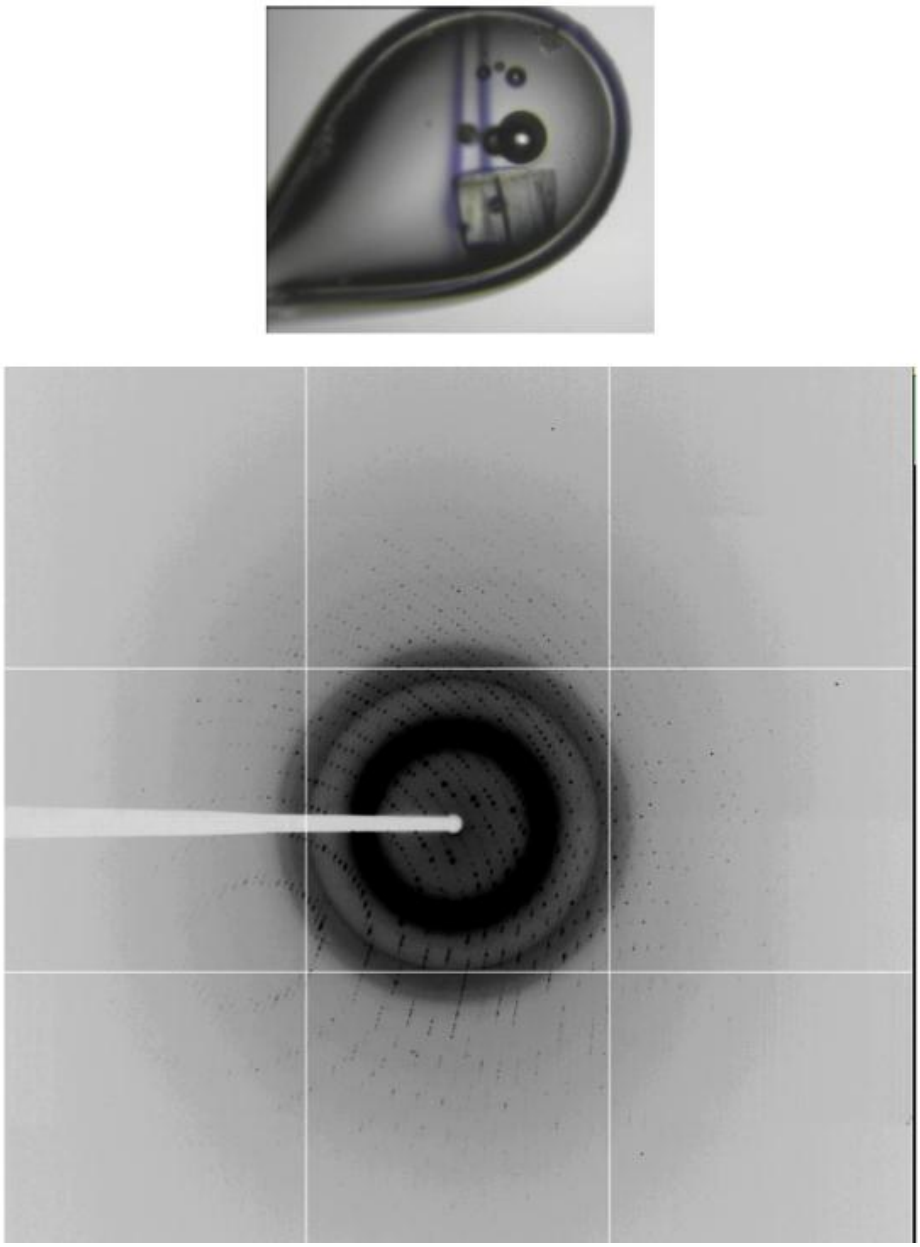

(Top) Picture of a frozen T.th. RuvC crystal in a nylon loop, taken after x-ray exposure. The vertical streak line marks the path of the x-ray beam. (Bottom) An x-ray diffraction image from the form I T.th. RuvC crystal. Diffraction spots extend to a ~1.2Å Bragg spacing.

Figure 3 | Structure of the T.th. RuvC monomer.

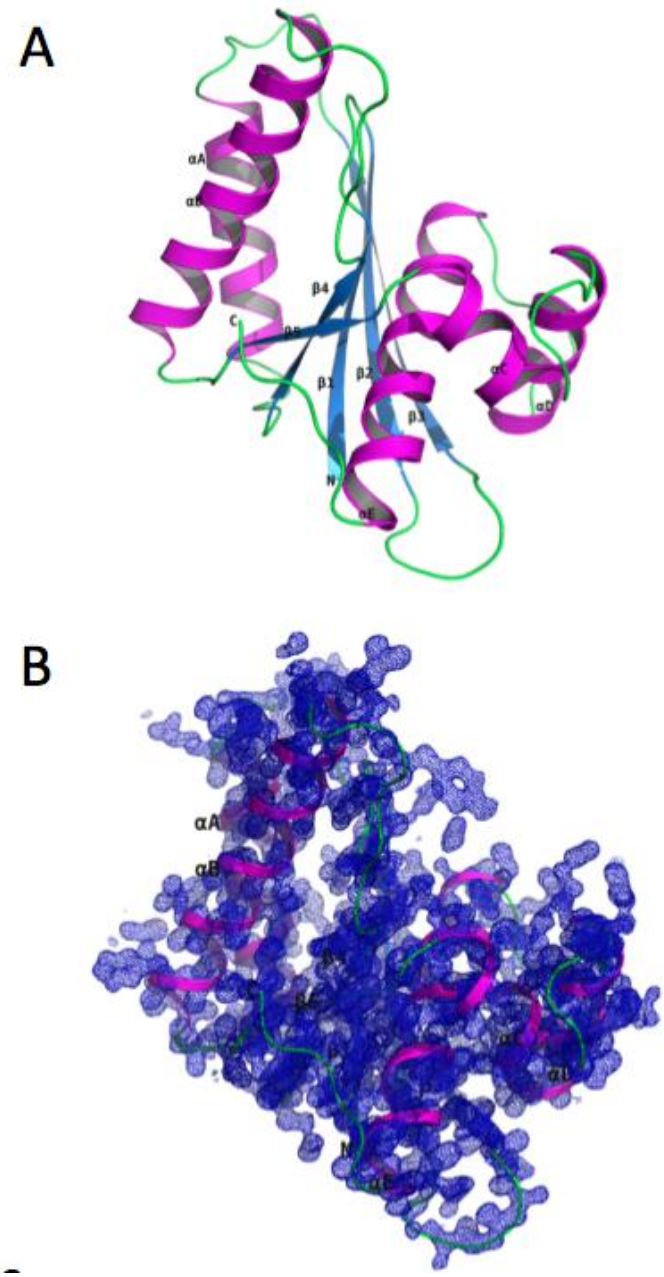

(A) T.th. RuvC monomer shown in a ribbom diagram, with the secondary structure elements labeled. (B) A σA-weighted 2Fo-Fc electron density map is overlaid on the ribbon diagram of the RuvC monomer.

Figure 4 | Comparison between the E. coli and T.th. RuvC.

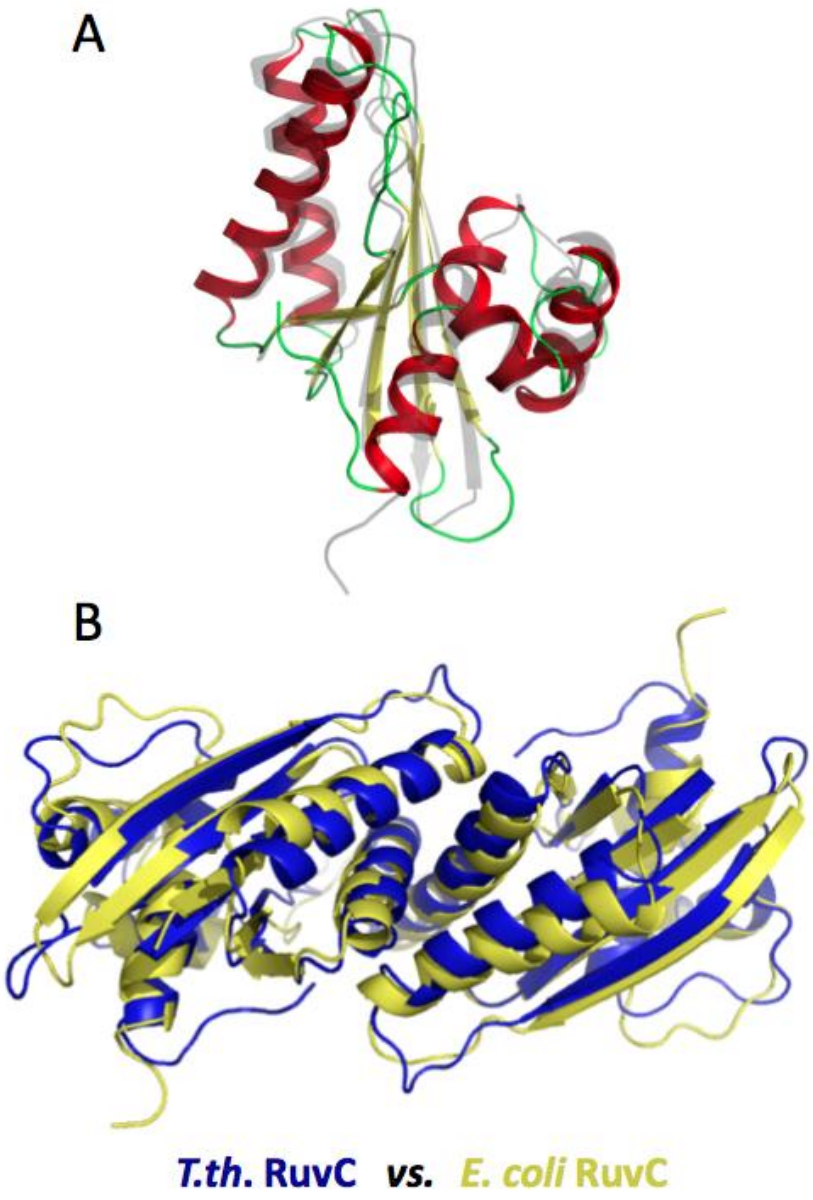

(A) T.th. RuvC monomer colored in red and yellow superimposed on the E. coli RuvC monomer in grey.

(B) T.th. RuvC dimer in blue superimposed on the E. coli RuvC dimer in yellow. Note that the α-helices are packed more tightly at the dimer interface in the T.th. RuvC dimer.

Figure 5 | The dimer interface of the T.th. RuvC dimer

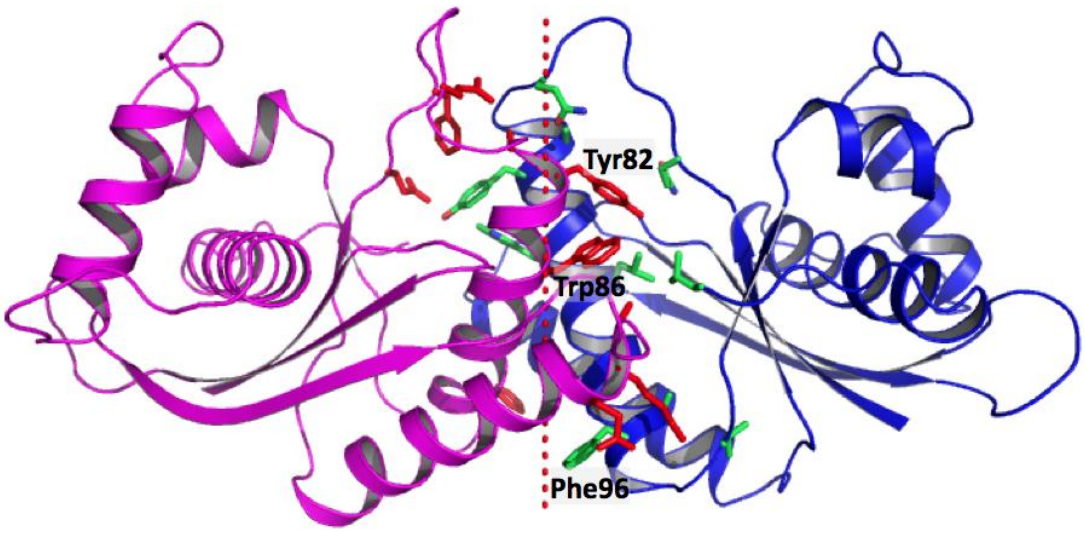

The aromatic residues Tyr82, Trp86, and Phe96 are labeled.

Figure 6 | The enzyme active site of T.th. RuvC

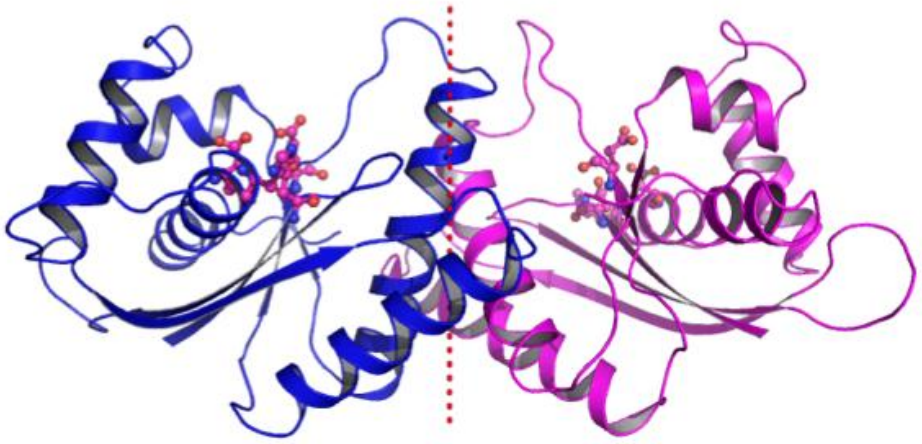

The active sites

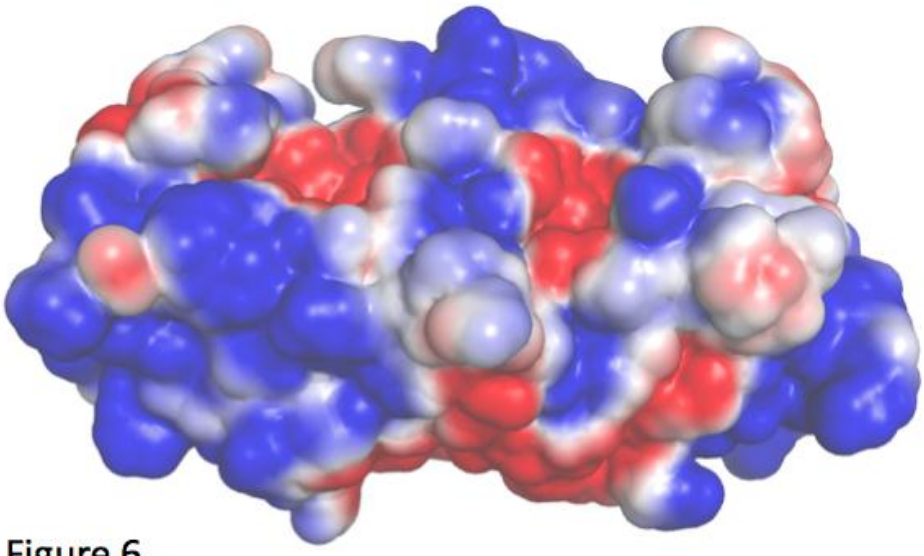

Figure 6

(A) Ribbon diagram of the T.th. RuvC dimer, with the catalytic residues Asp7, Glu70, His143, and Asp146 shown in sticks. (B) Electrostatic surface potential for the T.th. RuvC dimer. The active sites are negatively charged (red).

Figure 7 | T.th. RuvC-HJ model.

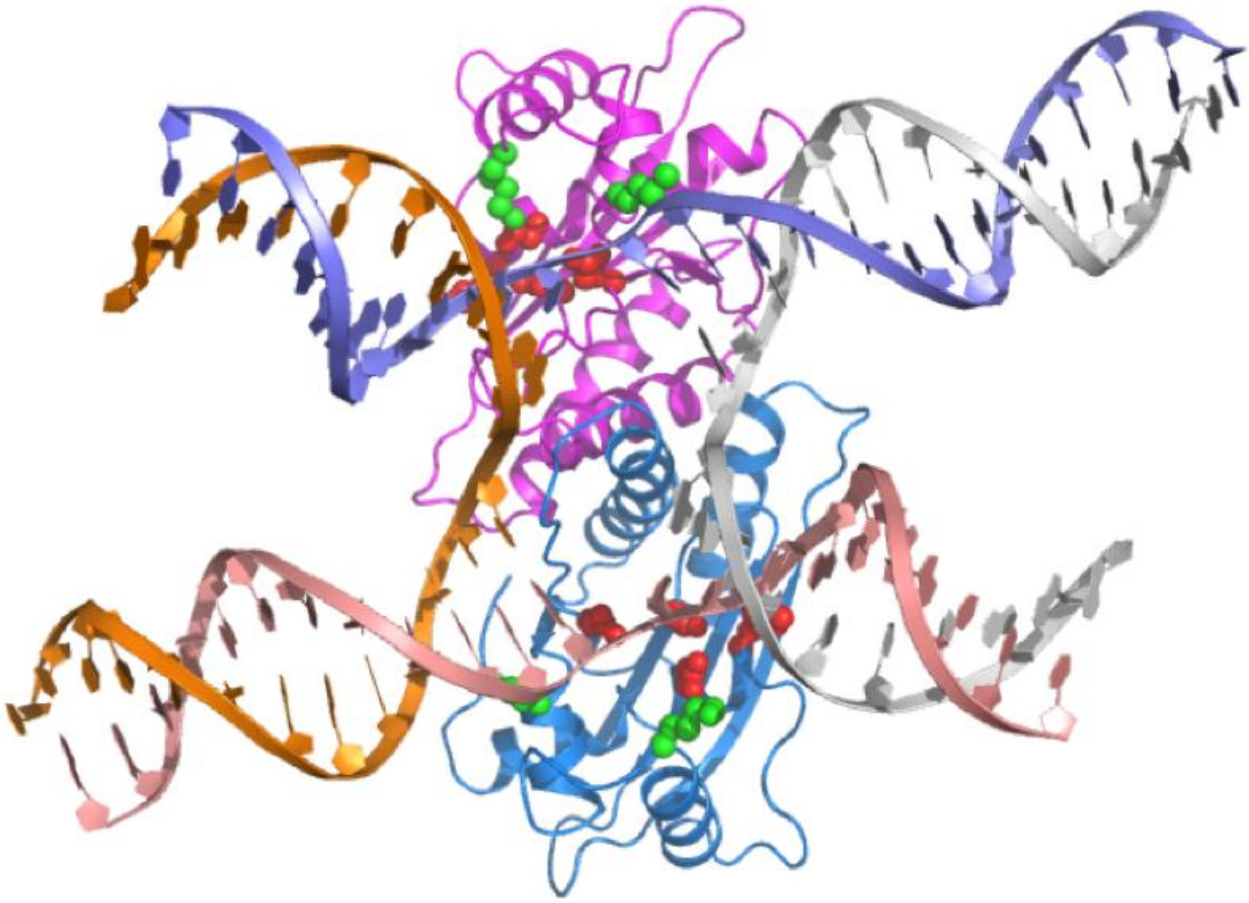

A hypothetical model of the T.th. RuvC dimer complexed with a HJ-DNA substrate.

Figure 8 | The asymmetric loop.

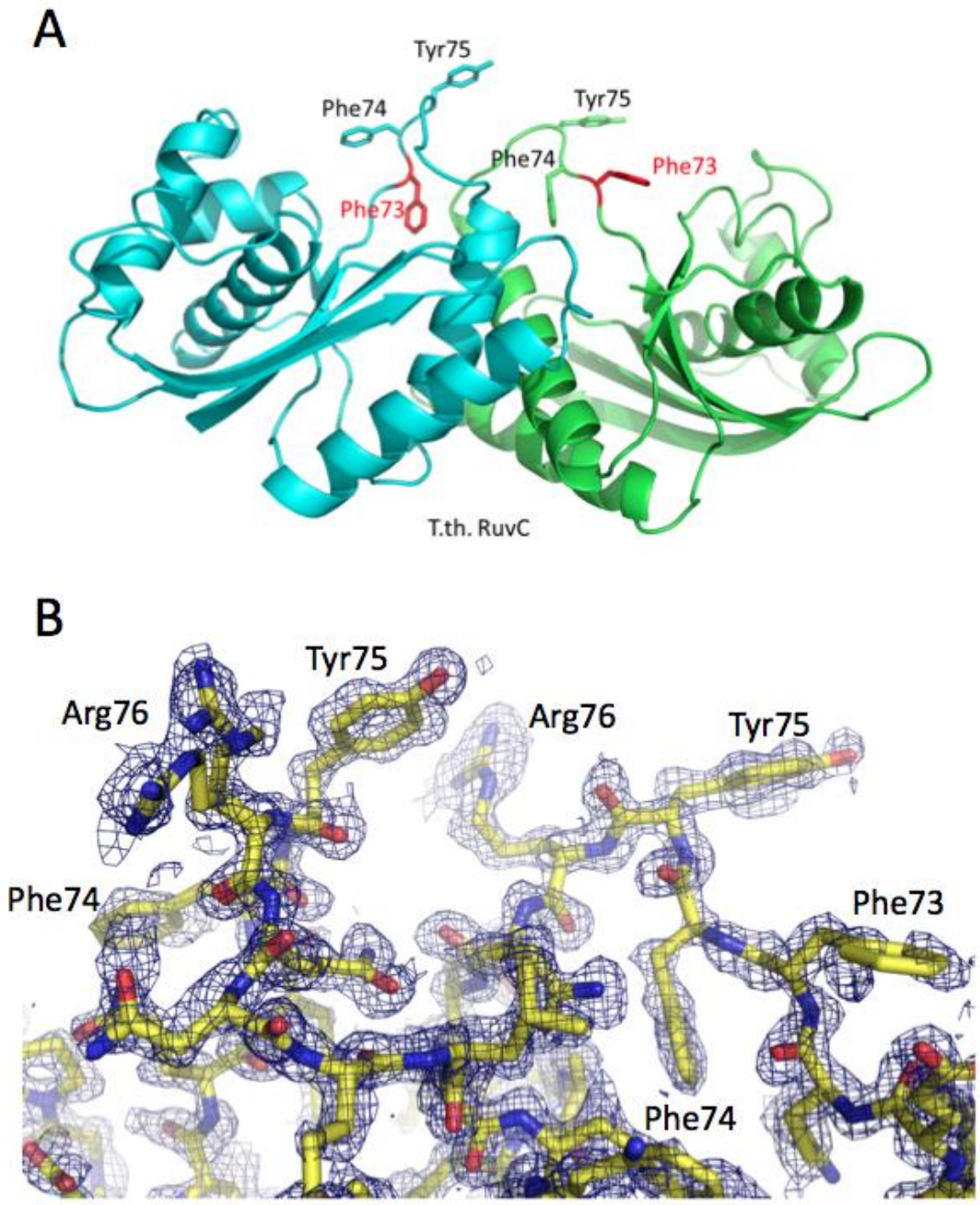

(A) Ribbon diagram of the T.th. RuvC dimer, with the aromatic residues in the asymmetric loop region Phe73, Phe74, and Tyr75 shown in sticks. (B) Electron density for the asymmetric loops. A simulated annealing composite omit map within 2.0Å from the protein atoms is shown, contoured at 1.0σ.